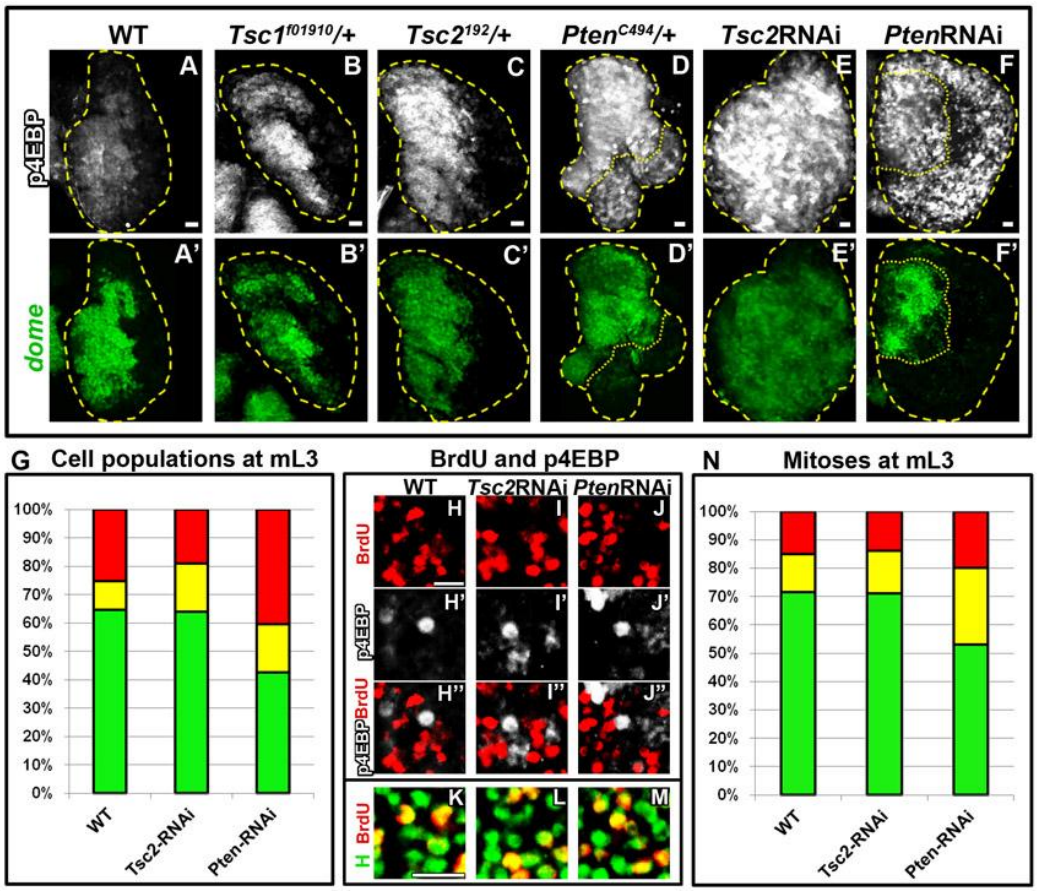

Fig. S1. Expression of p4EBP, cell population distributions and mitoses upon disruption of *Tsc1/2* and *Pten* function. (**A-F9**) Increase in p4EBP expression upon TORC1 pathway manipulation at wL3. Single-copy loss of *Tsc1* (*Tsc1*^{f01910}/+) (B,B9) or *Tsc2* (*Tsc2*^{192}/+) (C,C9) increases p4EBP expression (white) in *dome*$^{+}$ hemocyte progenitors (green), compared with WT (A,A9). Single-copy loss of *Pten* (*Pten*^{C494}/+) (D,D9) increases p4EBP expression both within *dome*$^{+}$ and *dome*$^{-}$ hemocytes. Downregulation of *Tsc2* (*dome*>*Tsc2*RNAi; E,E9) in hemocyte progenitors autonomously increases p4EBP expression in *dome*^{low} hemocytes throughout the LG. Downregulation of *Pten* (*dome*>*Pten*RNAi, F,F9) increases p4EBP autonomously within *dome*$^{+}$ hemocytes and non-cell-autonomously in *dome*-negative hemocytes. (**G**) Hemocyte and progenitor cell distributions at mL3 among the populations of *dome*$^{+}$/PXN^{-} prohemocytes (PH, green), *dome*$^{+}$/PXN^{+} intermediate progenitors (IP, yellow), and *dome*$^{-}$/PXN^{+} differentiated hemocytes (DH, red). WT LGs are composed of 65±5% PH, 10±3% IP and 25±5% DH. *Tsc2* downregulation in progenitors does not affect prohemocyte population size at mL3: 64±5% of the LG represents PH, whereas 17±3% of cells are IP and 19±6% are DH. *Pten* deficiency increases differentiation at the cost of prohemocytes: 43±8% of the LG represents PH, whereas 17±4% are IP and 40±9% are DH. Data are mean ± s.d. (*n*=10). Two-way ANOVA statistics showed significant changes (*P*<0.0001) in the distribution of hemocyte populations in *Tsc2*- or *Pten*-deficient LGs compared with WT at mL3. (**H-M**) Bromodeoxyuridine (BrdU, red) incorporation in WT (*dome*>*gal4*) (H-H0,K), *dome*>*Tsc2*RNAi (I-I0,L) and *dome*>*Pten*RNAi (J-J0,M) LGs at eL2. BrdU, a marker of cells in S phase, does not colocalize with p4EBP^{high} cells in any backgrounds (H-J0). Histone (H, green), a nuclear marker, overlaps with BrdU (red), indicating nuclear localization of BrdU (K-M). (**N**) Distribution of mitoses in mL3 LGs among the populations of *dome*$^{+}$/PXN^{-} prohemocytes (PH, green), *dome*$^{+}$/PXN^{+} intermediate progenitors (IP, yellow) and *dome*$^{-}$/PXN^{+} differentiated hemocytes (DH, red). In WT, 71.5±1.8% of mitoses occur in PH, whereas 13.5±3.4% occur in IP and 15±2.5% in DH. *Tsc2* downregulation does not affect the proportion of mitoses that occur in PH: 71±6.6% of mitoses occur within PH, whereas 15±5.3% occur in IP and 13.9±5.3% of mitoses occur in DH. By contrast, *Pten* downregulation decreases the proportion of mitoses in PH to 53.1±5.8%, whereas 27.1±5.3% of mitoses occur in IP and 19.8±7% in DH. Data are mean ± s.d. (*n*=10). Two-way ANOVA statistics comparing the distribution of mitoses at mL3 in *Tsc2*- and *Pten*-deficient LGs compared with WT showed no difference for *Tsc2*RNAi LGs (*P*>0.05), but a significant change upon *Pten* deficiency (*P*<0.0001). Scale bars: 20 μm in A-F; 10 μm in H-M.

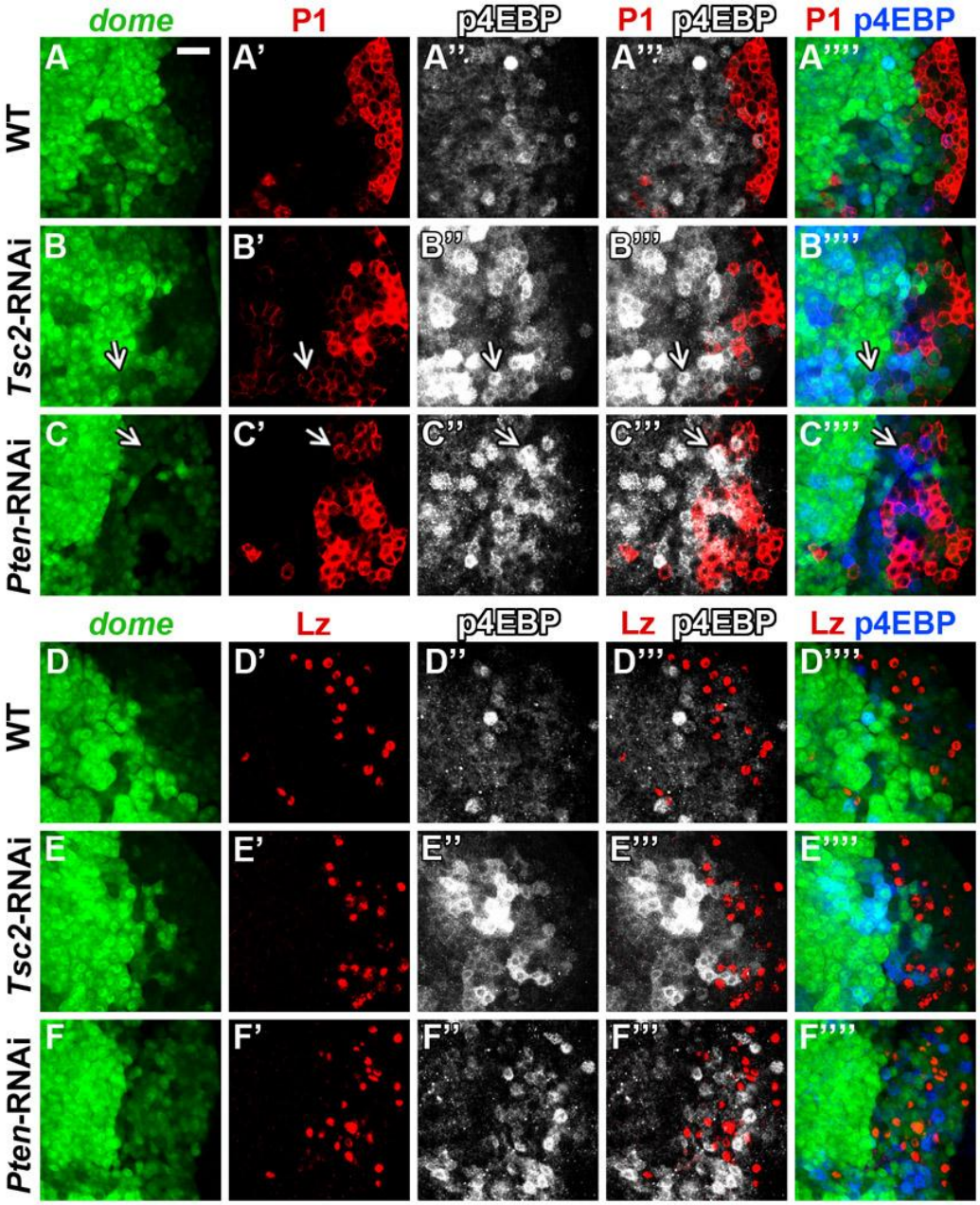

Fig. S2. Distribution of p4EBP^{high} cells in *Tsc2*- and *Pten*-deficient LGs at mL3. All panels represent mL3 LGs. p4EBP is shown in white in columns 3 and 4 and in blue in column 5. P1 (A-C−9) labels differentiated PLs, and LZ (D-F−9) labels CCs and their progenitors. L1^{+} lamellocytes were not observed at this stage in any of the genetic backgrounds. (**A-A-9**,**D-D-9**) WT. p4EBP is expressed throughout the primary lobe at low levels with some scattered p4EBP^{high} cells. A small population of P1^{+} (A-A−9) and LZ^{+} (D-D−9) hemocytes is present. (**B-B-9**,**E-E-9**) Downregulation of *Tsc2* (*dome*>*Tsc2*RNAi) expands the population of p4EBP^{high} cells. Rare p4EBP^{high} cells colocalize with P1^{low} (B-B−9) hemocytes (arrows), but not with P1^{high} hemocytes or with LZ^{+} cells (E-E−9). (**C-C-9**,**F-F-9**) Downregulation of *Pten* (*dome*>*Pten*RNAi) expands the population of p4EBP^{high} cells. A subset of P1^{+} hemocytes (arrows, C-C−9) are p4EBP^{high}, including some P1^{high} cells. LZ^{+} cells are often observed adjacent to p4EBP^{high} cells but they do not overlap (F-F−9). Scale bar: 20 μm.

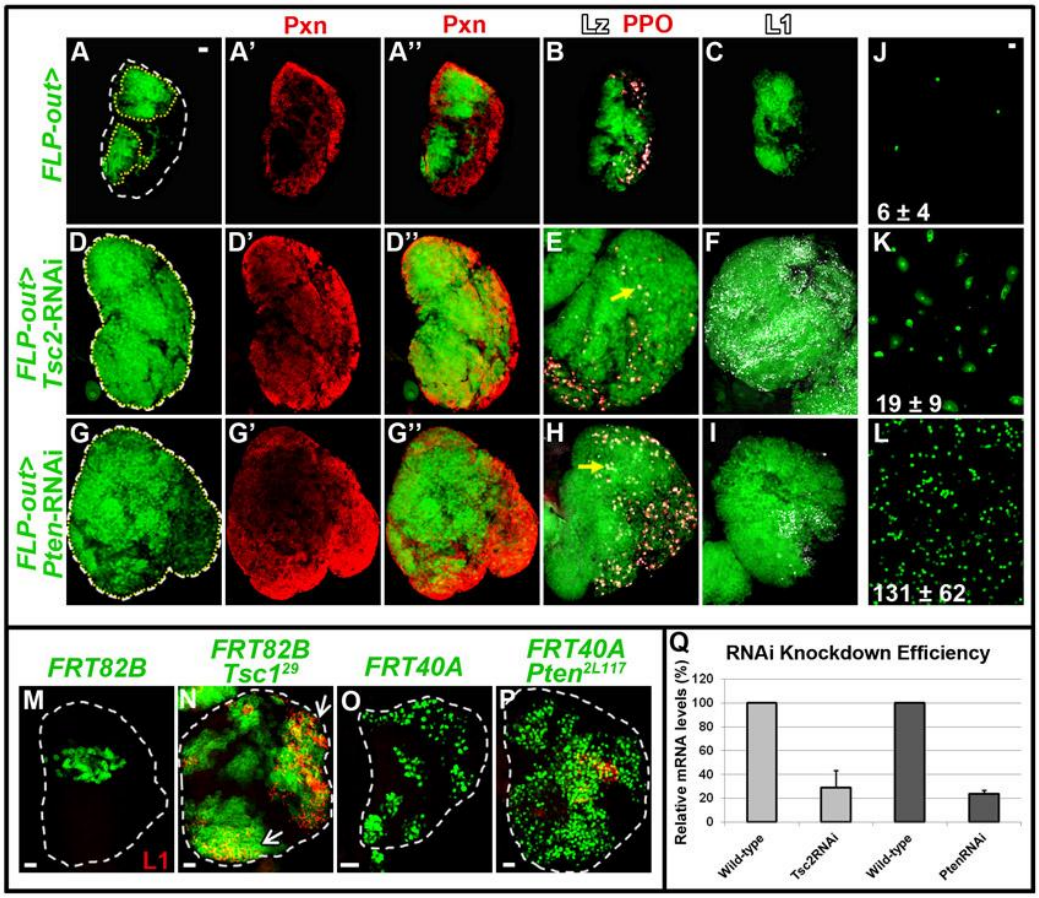

Fig. S3. Clonal analysis and knockdown efficiencies of *Tsc2*RNAi and *Pten*RNAi. Clones are demarcated in yellow in A,D,G. (**A-C**) WT LGs (*FLP-out*>): clonal expression of GFP (green) and normal expression of differentiation markers PXN (red, A9,A0), PPO (red, B), LZ (white, B) and L1 (white, C; not normally present in WT). (**D-F**) Clonal expression of *Tsc2*RNAi (*FLP-out*>*Tsc2*RNAi) increases LG size and GFP-marked clones encompass the entire LG lobe (compare with A-C). PXN (D9,D0) and L1 (F) expression expands throughout the LG. A small number of LZ^{+}/PPO^{-} CC progenitors (arrow) are also seen in medial regions of the LG (E), unlike in WT. (**G-I**) Clonal expression of *Pten*RNAi (*FLP-out*>*Tsc2*RNAi) increases LG size and increases differentiation (G9-H) with few lamellocytes observed (I). (**J-L**) Hemocyte bleeds from LG-specific lineage-traced larvae. GFP marks hemocytes in circulation that are derived from the LG. Very few LG-derived GFP^{+} hemocytes are observed in circulation in WT (J). Downregulation of *Tsc2* in the LG induces the release of LG-derived hemocytes, particularly lamellocytes, into circulation (K). Downregulation of *Pten* in the LG increases the relative number of LG-derived hemocytes, but not lamellocytes, released into circulation (L) compared with WT ($P<0.001$; J) or *Tsc2* downregulation ($P<0.001$; K). Data are mean ± s.d., $n=10$. (**M-P**) All panels represent wL3. MARCM clones for WT [*hs-flp FRT82B Tub-mCD8-GFP* (M) and *hs-flp FRT40A Tub-nGFP* (O)], $Tsc1^{29}$ (*hs-flp FRT82B* $Tsc1^{29}$ *FRT82B Tub-mCD8-GFP*, N) and $Pten^{2L117}$ (*hs-flp FRT40A* $Pten^{2L117}$ *FRT40A Tub-nGFP*, P). In WT, lamellocytes (red) are not observed (M,O). $Tsc1^{-/-}$ clones autonomously induce lamellocyte differentiation (arrows, N). $Pten^{-/-}$ clones induce a small number of lamellocytes (P). (**Q**) Knockdown efficiency of *Tsc2*RNAi and *Pten*RNAi constructs. Quantitative RT-PCR was performed to assess the relative levels of *Tsc2* or *Pten* at wL3, following ubiquitous expression of their respective RNAi constructs with *daughterless-Gal4*. Data are the mean of three replicates ± s.d. *Tsc2* mRNA transcripts were detected at 29.02% of WT, and *Pten* mRNA transcripts were detected at 23.88% of WT. Scale bars: 20 μm; except for 1.23 magnification for I.

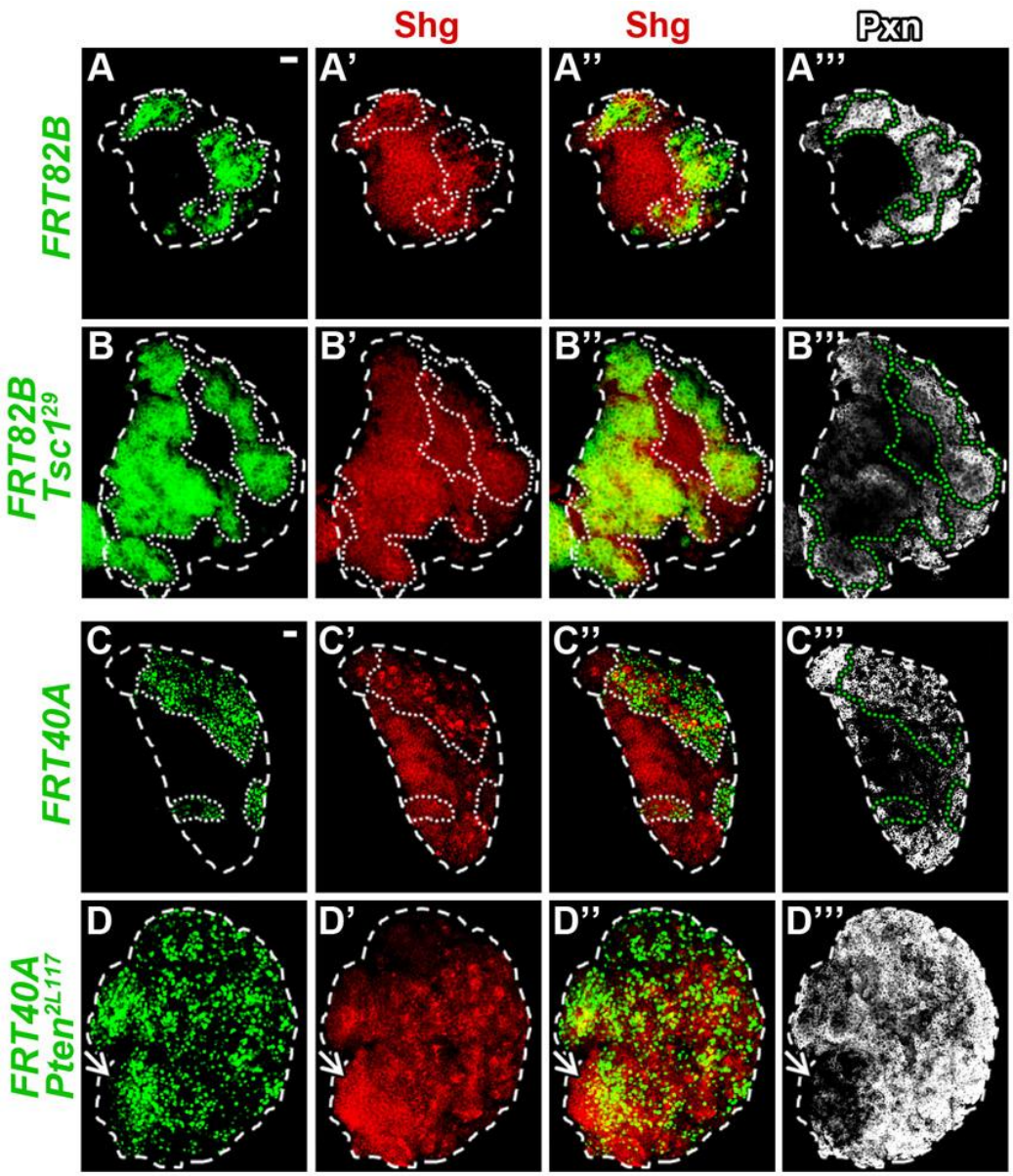

Fig. S4. Shotgun expression in *Tsc1* and *Pten* LOF backgrounds. All panels represent wL3. Clones are outlined by a white or green dotted line. (**A-B-**) *Tsc* MARCM clones. (A-A−) WT MARCM clones (*hs-flp FRT82B Tub-mCD8-GFP*). (B-B−) $Tsc1^{29}$ clones (*hs-flp FRT82B* $Tsc1^{29}$ *FRT82B Tub-mCD8-GFP*) maintain Shotgun (SHG, DE-cadherin) expression (red) in $Tsc1^{-/-}$ clones (green). High PXN expression (white) is observed only at the tissue periphery, while $Tsc1^{-/-}$ cells express low PXN levels (gray, B−). (**C-D-**) *Pten* MARCM clones. (C-C−) WT MARCM clones (*hs-flp FRT40A Tub-nGFP*) express highest SHG expression in medial, PXN-negative tissue. Cells in the periphery are differentiated and express reduced SHG levels, except for non-specific expression of SHG in scattered cells. (D-D−) $Pten^{2L117}$ clones (*hs-flp FRT40A* $Pten^{2L117}$ *FRT40A Tub-nGFP*) that are medially localized (arrow) are PXN negative and express high SHG levels. Scattered $Pten^{-/-}$ cells in the periphery are PXN^{high} (white) and express reduced levels of SHG, except for some scattered cells. Scale bars: 20 μm.

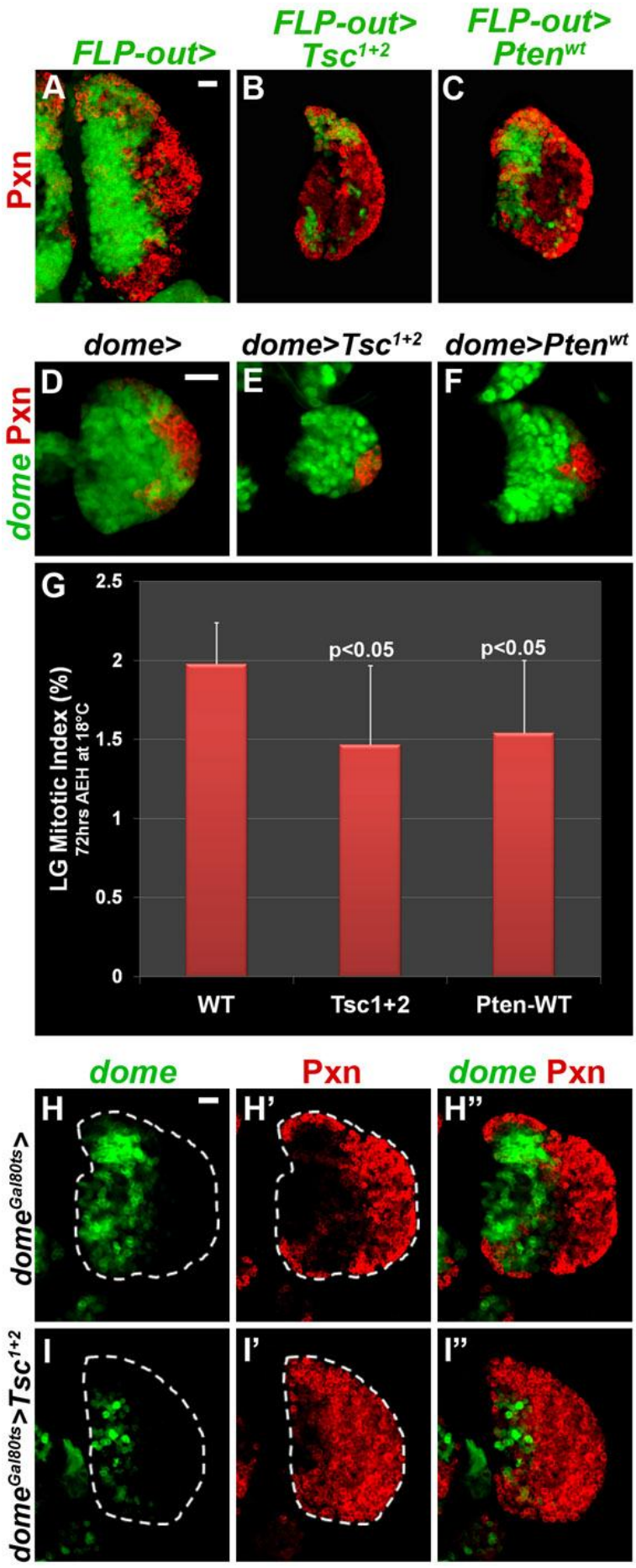
FLP-out>
FLP-out> Tsc1+2
FLP-out> Pten^wt
A
B
C
Pxn
dome>
dome>Tsc1+2
dome>Pten^wt
D
E
F
dome Pxn
G
LG Mitotic Index (%)
72hrs AEH at 18°C
2.5
2
1.5
1
0.5
0
p<0.05
p<0.05
WT
Tsc1+2
Pten-WT
dome
Pxn
dome Pxn
H
H'
H"
dome^Gal80ts>
I
I'
I"
dome^Gal80ts>Tsc1+2

Fig. S5. Inhibition of TORC1 signaling in prohemocytes impairs early LG growth. (**A-C**) FLP-out clones were generated specifically in the LG for WT (*FLP-out>*; A), Tsc^{1+2} (*FLP-out> Tsc^{1+2}*; B) and $Pten^{wt}$ (*FLP-out> $Pten^{wt}$*; C). Clonal overexpression of Tsc^{1+2} (B) or $Pten^{wt}$ (C) reduces overall LG size at wL3 and increases the population of PXN^+ hemocytes (red). (**D-F**) Overexpression of Tsc^{1+2} (E) and $Pten^{wt}$ (F) in prohemocytes decreases overall LG size at lL2, compared with WT (*dome>*, D), but the onset of differentiation of a small number of PXN^+ (red) hemocytes at the LG periphery occurs normally. Staging of *dome>Tsc^{1+2}* and *dome>$Pten^{wt}$* was performed at 18°C and lL2 larvae were dissected at 72 hours AEH. (**G**) Quantification of mitotic index at lL2. Overexpression of Tsc^{1+2} (1.47±0.5%, $P<0.0001$) or $Pten^{wt}$ (1.54±0.46, $P<0.0001$) in prohemocytes decreases mitotic index, compared with WT (1.98±0.26%). Data are mean ± s.d., $n=10$. (**H-I0**) Delaying expression of Tsc^{1+2} in prohemocytes until eL3 does not alter LG size (compare I0 with H0) but increases the number of PXN^+ differentiated hemocytes (red). Late expression of *UAS-Tsc^{1+2}* in progenitors was induced using *dome-gal4; P{tubP-gal80[ts]}20* and shifting larvae to the restrictive temperature (29°C) at eL3. Scale bars: 20 μm (for each row).

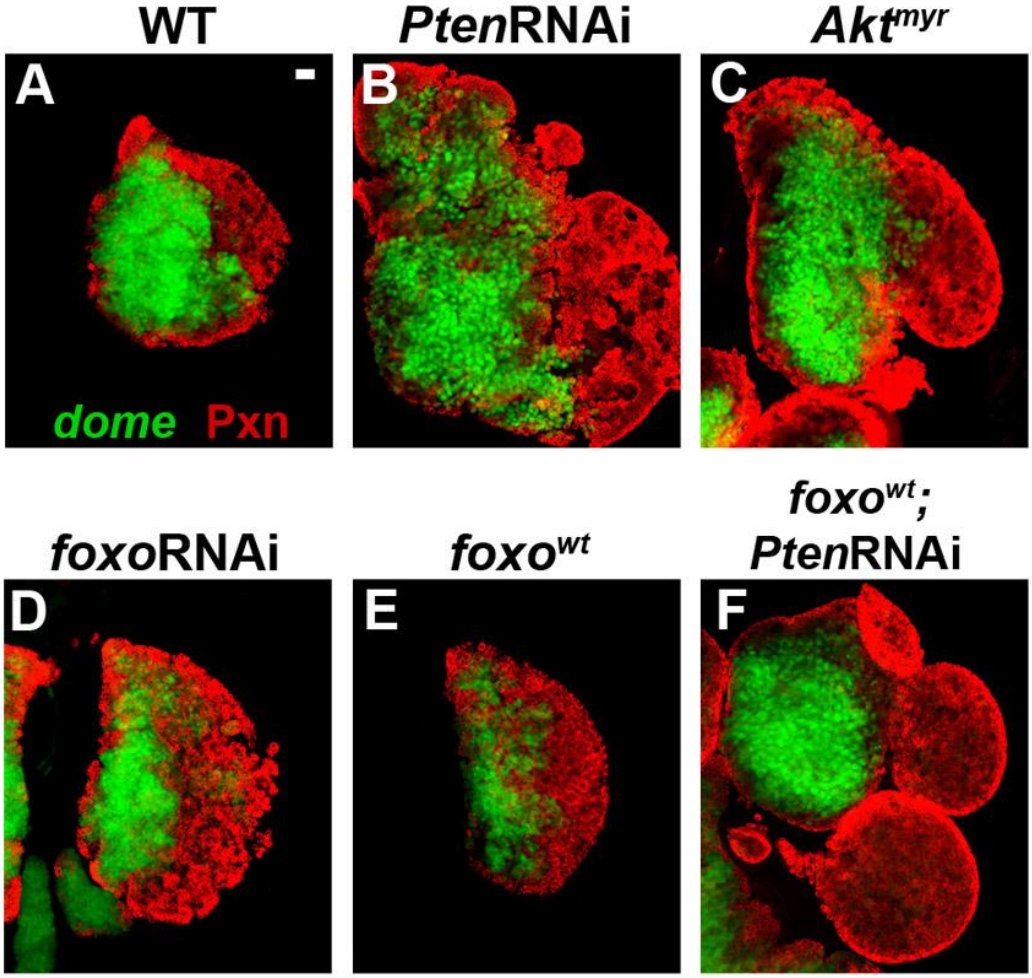

Fig. S6. FOXO-independent role of AKT in mediating *Pten* LOF phenotypes. All panels represent wL3 LGs. In all panels, *dome-gal4, UAS-2xEGFP* (green) drives expression of the genetic constructs listed. PXN expression is in red. (**A**) WT LG. (**B**) *Pten* downregulation in prohemocytes increases LG size and expands the population of PXN^+ hemocytes. (**C**) Overexpression of activated *Akt* (*Akt^{myr}*) increases the population of PXN^+ hemocytes, which sometimes 'bud' at the LG periphery. (**D**) Downregulation of *foxo* in prohemocytes does not phenocopy *Akt^{myr}* overexpression (C) or *Pten* downregulation (B) in the LG. (**E**) Overexpression of *foxo* increases PXN^+ hemocytes at the expense of prohemocytes. (**F**) Overexpression of *foxo* upon *Pten* downregulation does not rescue the accumulation of differentiated hemocytes associated with *Pten* deficiency (B). Scale bar: 20 μm.